Damage Detection of Wooden Beams Based on the Modal Strain Energy Change and Evidence Theory

Shaocheng Li,[a,]* Shanzhou Zeng,[a] Chenkan Jiang,[a] Guangzhou Xu,[a] Zhao Zhang,[a] and Qinjie Sun [b]

A damage detection and localization method for wooden beams was proposed based on the modal strain energy (MSE) change and evidence fusion. The fused damage indicator was deduced using the first three mode shapes of the wooden beams before and after damage. The finite element modal analysis of the free-supported undamaged and damaged wooden beams with different damage severities at one or two locations was performed. The first three mode shapes were extracted from the corresponding modal analysis, with which the damage indicator based on the MSE change and the fused damage indicator of each damage case were computed. The simulation results show that the fused damage indicator accurately detected and located the damage with different severities at one or two locations. Finally, the modal test was completed using the same damage cases as the finite element simulation. The frequency functions of the whole beam were first obtained, with which the first three experimental mode shapes were then acquired, and the damage indicator based on the MSE change and the fused indicator were further computed. The test results verified the validity and reliability of the proposed damage indicator.

DOI: 10.15376/biores.18.3.5133-5145

Keywords: Damage detection; Wooden beam; Modal strain energy; Evidence theory

Contact information: a: College of Materials Science and Engineering, Nanjing Forestry University, Nanjing, 210037 China; b: Nanjing Sanle Group Co., Ltd., Nanjing, 211800 China;
** Corresponding author: shaochengli@njfu.edu.cn*

INTRODUCTION

Given environmental exposure and mechanical loading, a wooden structure is subjected to damage such as rot and cracks. This local damage will reduce the structure's mechanical properties and affect its safety and integrity. Damage detection on the weak location of the structure should be completed to avoid casualties and heavy economic losses (Hu *et al.* 2011). Vibration-based methods have increasingly been applied for detection of structural damage, on account of their non-destructive character and cost-effectiveness. Through analyzing the frequency response functions according to the vibration excitation and response signals of a structure, its modal characteristic parameters (*e.g.*, natural frequencies and modal shapes) can be obtained, and its local damage can be detected based on the change of modal characteristic parameters (Teng *et al.* 2019). Some research results showed that indicators based on mode shapes were more ideal and accurate than those based on mode frequencies for locating and estimating the size of damage in beam-type structures (Pandey *et al.* 1991; Kim *et al.* 2003). Over the past 20 years, some researchers have introduced the vibration-based method into local damage detection for wooden beams.

Some damage indicators based on mode shapes, mode curvature, or statistic algorithms have been proposed for detecting and locating local damage with different severities, locations, and numbers in wooden beams (Yang *et al.* 2002, 2003; Hu and Afzal 2006). An improved damage detection algorithm by modal strain energy was attempted to accurately detect and locate the local damage for wooden beams (Choi *et al.* 2007). Modal strain energy (MSE)-based damage identification methods have been successfully applied to machinery, bridges, and other projects to achieve damage detection and localization (Shi *et al.* 1998; Liu *et al.* 2017; Ghiasi *et al.* 2018; Wang and Xu 2019; Khosravan *et al.* 2021). However, for a wooden beam, some signal noise was noticed within the captured mode shapes in practice; thus, locating the structural damage remains a challenge. The data fusion method has good anti-noise ability and can effectively improve the accuracy of damage identification by information complementarity (Zhang *et al.* 2022). Some researchers have applied evidence theory to damage localization, and the results verified the effectiveness of the fusion method based on evidence theory (Fei *et al.* 2009; Qin *et al.* 2020). However, to date, research on the damage detection of wooden beams based on the fusion method of the MSE change and evidence theory is minimal.

This study proposes a fused damage indicator based on the modal strain energy change and evidence theory to improve the accuracy of damage detection and localization for wooden beams. The feasibility and validity of the proposed damage indicator were first confirmed by the finite element simulation analysis of wooden beams and then further verified by the modal experiments.

EXPERIMENTAL

Material and Equipment

The test materials were four groups of uniform wooden beams without any defects cut from a log of *Pinus sylvestris*. The beam dimensions were 2000 mm × 40 mm × 80 mm (length × width × height) with a moisture content of approximately 12%, an average density of 550 kg/m^3, a longitudinal elastic modulus of 7500 MPa, and a Poison's ration of 0.35. Each sample beam was marked as 50 equal elements along its length, and each element was called a node. The damaged beams were made by removing mass from the intact wooden beams. Several kinds of damage scenarios were simulated, including single and dual defects, as listed in Table 1. Each scenario was a rectangular gap at the center of a node on top of the sample beam, as shown in Fig. 1. The width of each gap was kept constant at 4 mm, whereas the depth of the gaps was 10%, 30%, and 50% of the beam height, respectively, corresponding to three kinds of damage severities: light (*L*), middle (*M*), and serious (*S*). According to the loss of the moment of inertia, the damage degree φ is expressed as follows,

$$\varphi = 1 - \frac{\frac{b(\mathrm{h}-h_1)^3}{12}}{\frac{bh^3}{12}} * 100\% = \frac{{h_1}^3 - 3h{h_1}^2 + 3h^2 h_1}{h^3} * 100\% \qquad (1)$$

where h_1 and h are the depths (mm) of the gap and the wooden beam, respectively.

The modal simulation analysis was completed with ANSYS software (version 14.0, NASDAQ: ANSS, Pittsburgh, PA, USA). The test instruments included a set of vibration excitation and dynamic signal acquisition and analysis systems, containing an impact hammer (INV9311, Dongfang Institute of Vibration and Noise Technology, Beijing, China) with an IEPE pressure sensor with a measurement range of 0 to 550 N and a sensitivity of 7500 mV/N; an IEPE acceleration sensor (INV9822, Dongfang Institute of Vibration and Noise Technology, Beijing, China) with 50 g in mass, a sensitivity of 100 mV/g, and a frequency response range of 0.5 to 8000 Hz; a data acquisition card (NI PXIe-4496, National Instruments, Austin, TX, USA) with a 24-bit analogue-to-digital converter with a sampling rate of up to 204.8 KS/s per channel and 16 available channels for simultaneous measurement; and its controller (NI PXIe-8133, National Instruments) installed in the chassis (NI PXIe-1075, National Instruments). The software for dynamic signal acquisition and analysis was programmed in LabVIEW (version 2011, National Instruments, Austin, TX, USA).

Table 1. Damage Cases of Wooden Beams

Case	Scenario	Location (Node)	Width (mm)	Depth (h_1/h)	Damage Degree (%)
1	25*L*	25	4	1/10	27.1
2	25*M*	25	4	3/10	65.7
3	25*S*	25	4	5/10	87.5
4	13*L*	13	4	1/10	27.1
5	33*L*	33	4	1/10	27.1
6	25*M*, 33*L*	25, 33	4	3/10,1/10	65.7 and 27.1
7	25*M*, 33*M*	25, 33	4	3/10,3/10	65.7 and 65.7
8	25*M*, 33*S*	25, 33	4	3/10,5/10	65.7 and 87.5

Fig. 1. Rectangular gap of a sample beam

Theory and Method

Damage indicator based on the MSE *change*

Suppose there are n elements in the beam along the length direction. For the j^{th} element and the i^{th} vibration mode of the undamaged and damaged beam, the element modal strain energy MSE_{ij}^{u} and MSE_{ij}^{d} can be defined, respectively, as follows (Khosravan *et al.* 2021),

$$MSE_{ij}^{u} = \emptyset_{ui}^{T} K_j \emptyset_{ui} \tag{2}$$

$$MSE_{ij}^{d} = \emptyset_{di}^{T} K_j \emptyset_{di} \tag{3}$$

where $\emptyset_{ui}$ and $\emptyset_{di}$ are the i^{th} mode shapes of the undamaged and damaged beam, respectively, and K_j is the stiffness matrix of the j^{th} element of the undamaged beam.

Because the degree and location of the damage to the damaged beam are unknown, K_j is also used in Eq. 3.

According to the above equations, the damage index developed by Choi was adopted and modified as follows (Choi *et al.* 2007),

$$MSEI_{ij} = \frac{\left(MSE_{ij}^{d}+MSE_{i}^{d}\right)\times MSE_{i}^{u}}{\left(MSE_{ij}^{u}+MSE_{i}^{u}\right)\times MSE_{i}^{d}} - 1, \tag{4}$$

where MSE_i^u and MSE_i^d are the modal strain energies (J) of the i^{th} vibration mode of the undamaged and damaged beam, respectively.

To reduce the error influence caused by single-order mode shape, multi-order mode shapes are generally used for the damage indicator. In the actual detection of wooden beams, although some noises are detected in the first three mode shapes, the data quality of the mode shapes of the fourth order and above is poorer. Thus, the first three mode shapes were selected for the calculation of the damage indicator, as follows,

$$MSEBI_j = \frac{1}{3}\sum_{i=1}^{3} MSEI_{ij}, \tag{5}$$

where $MSEBI_j$ is the damage indicator based on the MSE change for a single element *j*.

Fused damage indicator based on the MSE *change and evidence theory*

Dempster-Shafer (DS) evidence theory, which was developed by Dempster and Shafer (Qin *et al.* 2020), which can fuse data from multiple information sources and improve the accuracy of damage identification. The *n* elements in the beam serve as subsets in DS evidence theory. After the indexes of modal strain energy of *n* elements were obtained by Eq. 4, the basic probability for each element can be calculated as follows,

$$m_i(j) = \frac{MSEI_{ij}}{\sum_{j=1}^{n} MSEI_{ij}} \tag{6}$$

where $m_i(j)$ is the probability assignment for the j^{th} element and the i^{th} vibration mode.

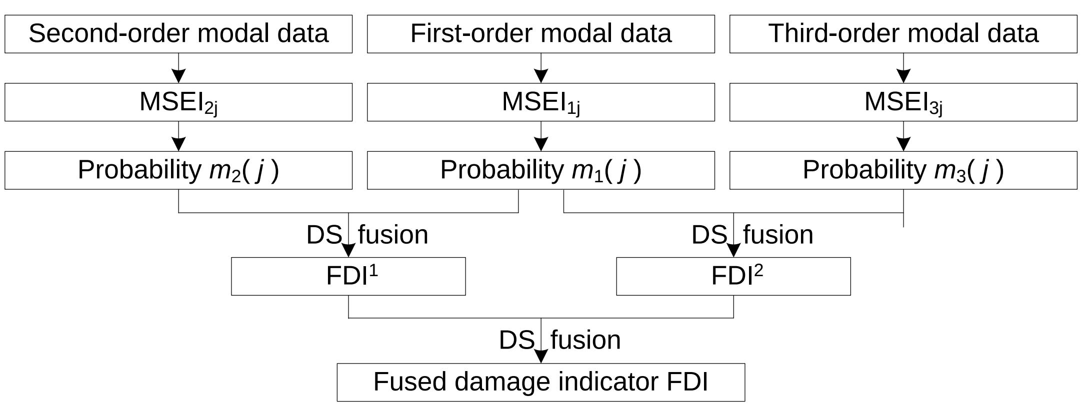

Fig. 2. Flowchart of damage index fusion process

For $m_i(j)$ (i = 1, 2; j = 1, 2… n), DS fused results can be computed following Eqs. 7 and 8,

$$m(j) = \frac{m_1(j) * m_2(j)}{K} \tag{7}$$

$$K = \sum_{j=1}^{n} m_1(j) * m_2(j) \quad (8)$$

where $m(j)$ is the fused damage indicator (FDI).

For the actual first three mode shapes, the data quality of the first-order mode shape is better than that of the second-order and third-order mode shapes. Therefore, the fusion method focusing on the first-order mode shape is proposed, which is shown in Fig. 2.

RESULTS AND DISCUSSION

Verification of the Effectiveness of the Proposed Damage Indicator Based on Finite Element Analysis

Timber is an orthotropic material with different mechanical properties along the longitudinal, radial, and tangential directions. Wooden beams are cut from logs along the length. Thus, they have the same mechanical properties as timber and have three Young's moduli E_1, E_2, and E_3; three shear moduli G_{12}, G_{13}, and G_{23}; and three Poisson's ratios. The simulation work of Kouroussis *et al.* (2017) found that the bending mode shape of wooden beams depended mainly on the parameter of E_1, and other parameters had negligible influence. Thus, the wooden beam can be regarded as an isotropic material for the parameter extraction of the bending mode shape in finite element modal analysis.

The finite element three-dimensional model of the free-supported wooden beam was established by ANSYS software according to the above material parameters and size. Each model of the damaged beams was constructed by removing the same volume and shape as that of Table 1. The model of Case 2 in Table 1 is shown in Fig. 3. To reduce operation time and assure the accuracy of modal analysis, the model was meshed with a solid shell element at the mesh size of 0.02 m, and the dynamic simulation was limited to the linear elastic range. The first three mode shapes should be output in the modal analysis for each model, including the damaged and undamaged wooden beams.

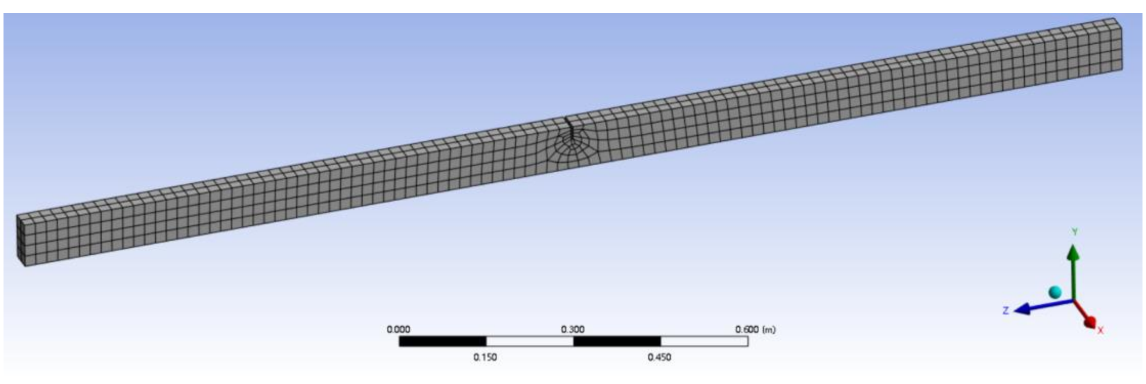

Fig. 3. Finite element model of Case 2

Each sample beam was regarded as 50 nodes in the follow-up modal test. To maintain consistency with the experimental data, 50 points of data that corresponded to the center points of the beam nodes were extracted from the result of finite element modal analysis for each of the first three mode shapes. The first three mode shapes for the model of Fig. 3 are shown in Fig. 4.

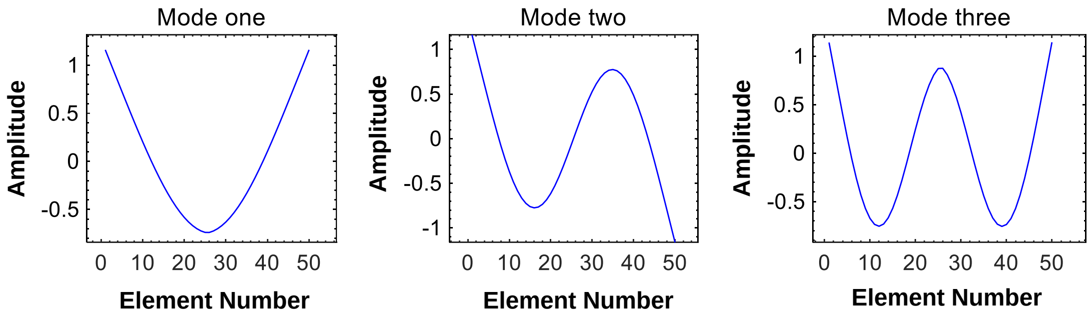

Fig. 4. The first three mode shapes of Case 2

Based on the first three modal data, the damage indicator based on the MSE change (MSEBI) and the fused indicator were computed by the above equations, and the detection results are shown in Figs. 5 and 6. Figure 5 shows the detection results of single damage with different severities at the same location. The figure indicates that the damages of different degrees can be detected and located accurately by these two methods and the two damage indicators ascend with increasing damage severity. For the MSEBI results in Fig. 5(a), the peak values increase from 0.0073 and 0.0707 to 0.2143, with the damage degree increasing from *L* and *M* to *S*, which suggests that the peak values of MSEBI indicators are sensitive to the different damage severities. Through comparing the results of the two indicators in Fig. 5, the peak values of the evidence fusion indicator increase correspondingly from 0.0073, 0.0707, and 0.2143 to 0.8471, 0.9053, and 0.9522, which are much larger than those of the MSEBI indicator.

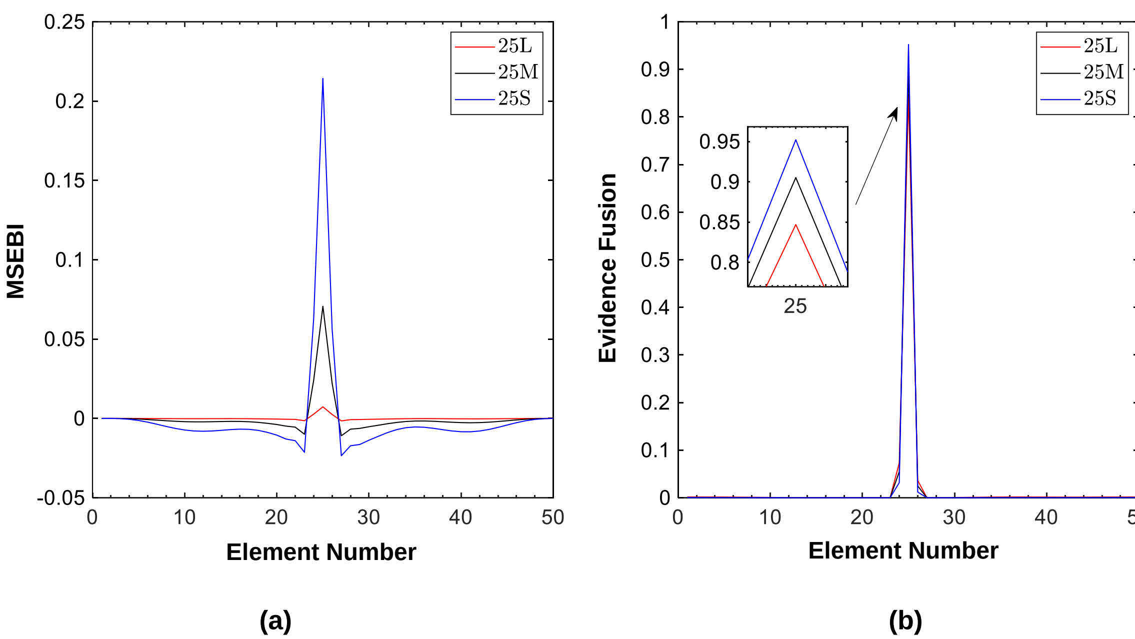

Fig. 5. The detection results of single damage with different severities at the same location (a) MSEBI; (b) Evidence fusion FDI

Figure 6 shows the detection results of single damage with the same damage severity at different locations. It is shown that these two indicators can also correctly detect and locate damages at different locations. Despite the same damage severity, the peaks of the indicators at different locations are different. The reason for this phenomenon is that the modal shapes are the cumulative function of the vibration displacement (Hu *et al.* 2011). It can be seen from Fig. 4 that the values of the first three mode shapes change with the location along the beam. Based on Figs. 5 and 6, damages to wooden beams can be accurately detected and located using the two indicators for ideal shape data without noise. However, the peak value of the MSEBI indicator is much smaller, and some fluctuations are observed in the MSEBI indicators, which are susceptible to noise, whereas the fused indicator is more accurate and reliable in damage detection and localization.

Figure 7 shows that dual damages with different severities at different locations can be correctly detected and located with the fused indicator. However, the peaks of the fusion indicators for relatively light damage become smaller compared with single damage detection. This phenomenon arises because the fusion method amplifies the difference of the damaged data based on MSEI. That is, the probability of damage with major severity is amplified, whereas the probability of the indicator of the damage with minor severity is relatively small, which also illustrates that the fusion method can effectively resist noise.

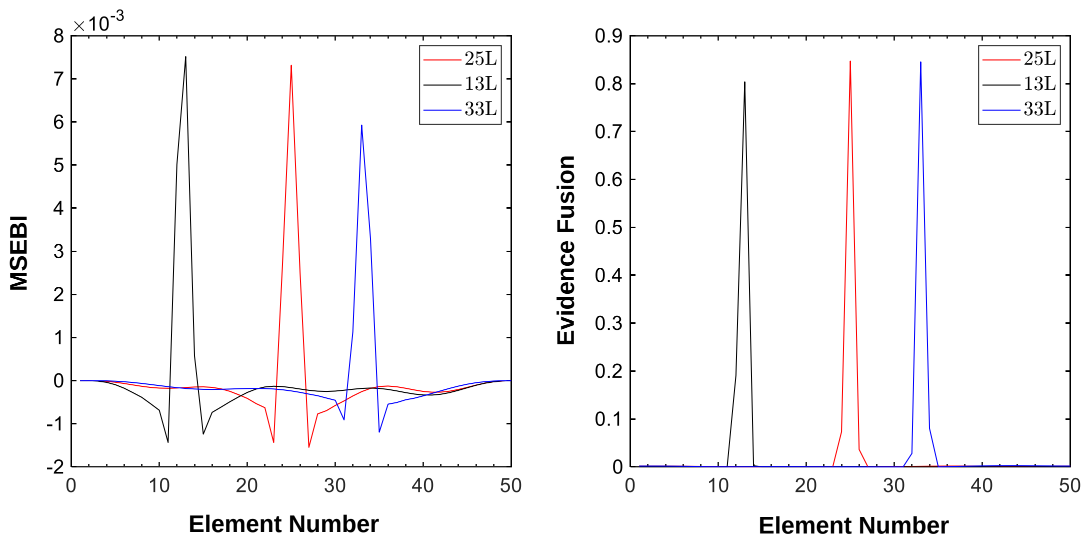

(a) **(b)**

Fig. 6. The detection results of single damage with the same severity at different locations (a) MSEBI; (b) Evidence fusion FDI

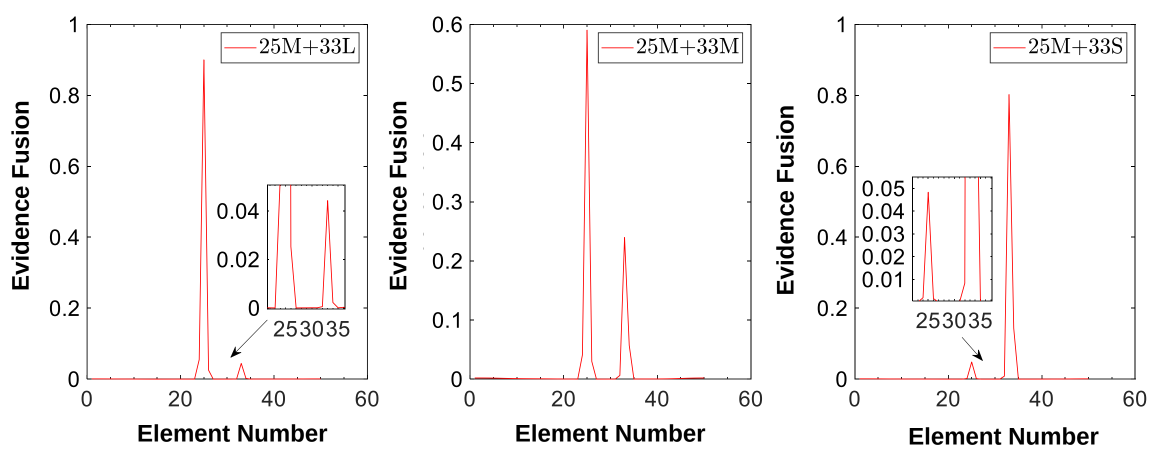

Fig. 7. The detection results of dual damages based on the evidence fusion FDI

Verification of the Effectiveness of the Proposed Damage Indicator Based on the Modal Test

Test principle and method

In the modal test, the beam is regarded as several uniform elements, and the frequency function of each element is acquired by the hammering method. Using the frequency functions of the whole beam, the modal parameters of each beam can be obtained based on the rational fraction polynomial method. The frequency functions of the whole beam can be obtained in two ways. One way is to use one beam element as an impact point and place sensors on other elements, in which way a single impact can obtain all of the frequency functions. The other way is to place one sensor on the center of the top surface of one element and impact on the center points of the top surfaces of other elements singly, in which way more impact points are available. The first method needs many sensors, and the mass of the sensors may affect the modal parameters of the beam. Thus, the second method was employed.

For reconstructing the mode shapes, the more elements the sample beam is divided into, the more accurate the modal shape will be. However, too many elements can lead to difficulties in the actual operation. Thus, in the actual modal test, the precision of mode shape and ease of operation were comprehensively considered. Each sample beam was divided into 50 elements; one element was used to attach the sensor, and other elements were used as impact points. The test block diagram is shown in Fig. 8. The sample beam was suspended from the fixed supports *via* the elastic ropes, and the acceleration sensor was firmly attached to the top surface center of a certain element, which is not zero points of the first three vibration modes.

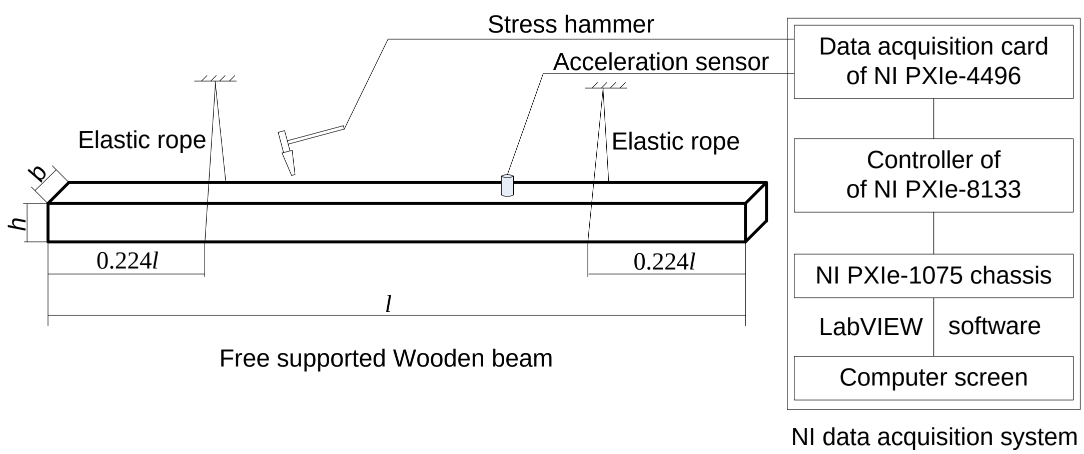

Fig. 8. Schematic diagram of the detection system

The acceleration and pressure sensors of the stress hammer are all of IEPE type and can be directly corrected to the data acquisition card. The data acquisition card was especially used for vibration signal acquisition designed by National Instruments and can supply 4 mA current for the sensors. Based on the software of LabVIEW, the signal acquisition system was programmed by the DAQmx functions, and it can capture signals from the acquisition card by the controller. The sampling rate was set to 2000 Hz, and the number of sampling points was 6000. The signal acquisition of the acceleration sensor was triggered by the impact signal of the stress hammer. When the top surface center of each element of the sample wooden beam was excited by the stress hammer, the signal acquisition system recorded the signals of the two sensors simultaneously. The frequency function was obtained based on the two sensors' time signal. The modal parameters of the sample beams were further obtained based on the frequency functions of 50 elements. The experimental device is shown in Fig. 9.

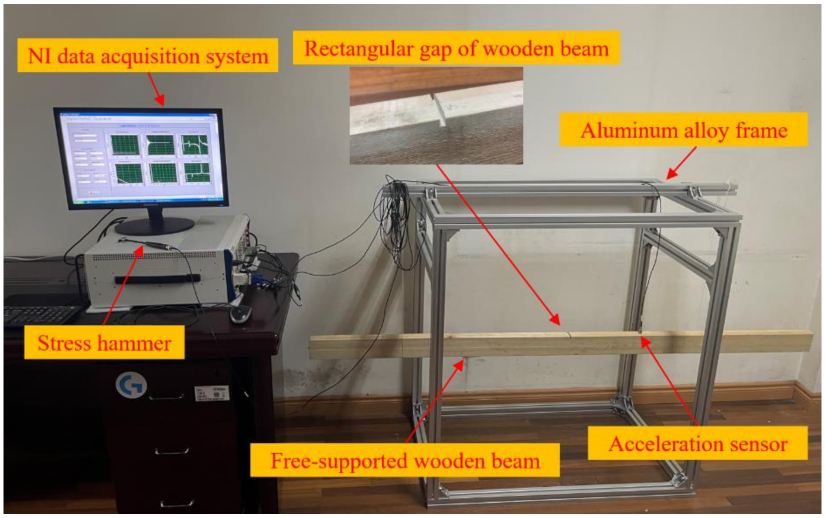

Fig. 9. The experimental device

Damage detection and localization

Based on the modal shapes obtained from the tests, the MSEBI indicators were computed by Eq. 5, and the evidence fusion indicators were further obtained by Eq. 7. The detection results based on the test data are shown in Figs. 10, 11, and 12. The detection results of the damage with different severities at the same location are depicted in Fig. 10, which shows that the FDI indicators can accurately detect and locate the damage with different severities. However, the MSEBI indicators show several tiny false peak points, which may cause wrong damage detection and localization. The reason for this phenomenon is that the peak values of MSEBI indicators are smaller and more susceptible to noise.

Figure 10(a) also shows that the main peak values of MSEBI indicators are sensitive to different damage severities, the same as the finite element simulation results, which can be seen in Table 2. The main peak values ascend with the damage degree increasing from *L* and *M* to *S*. However, the damage severity cannot be quantitatively distinguished by the MSEBI indicator. Figure 11 describes the detection results of the damage with the same severity at different locations. Several tiny false peak points are observed in the MSEBI indicators, which may cause wrong damage detection and localization. The detection results based on the evidence fusion indicator in Fig. 11(b) further verified the validity of the fusion method. The indicator peak of the damaged element is apparent, and its peak values of different damage locations are all above 0.45, whereas the indicator values of undamaged elements are all near zero.

Figure 12 gives the detection results of the dual damages with different severities, clarifying that the damages with different severities at the two locations can be accurately detected and located, which further confirms the validity and reliability of the proposed damage detection method.

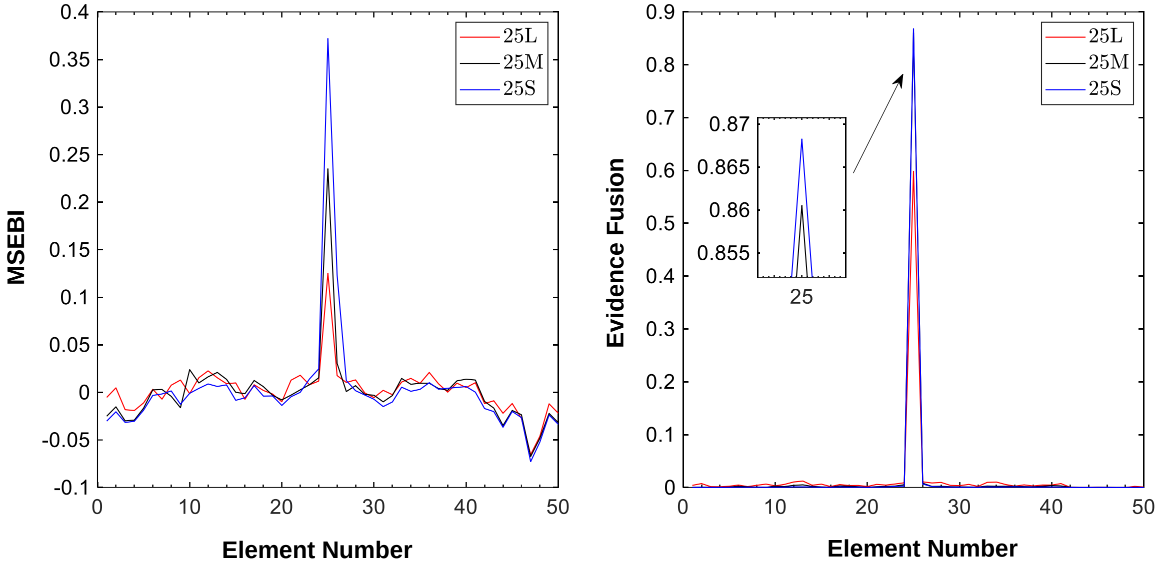

(a) (b)

Fig. 10. The detection results of single damage with different severities at the same location (a) MSEBI; (b) Evidence fusion FDI

Table 2. Identification of Single Damage at the Same Location

Case	Scenario	Main Peak Value of MSEBI	
		Finite Element Analysis	Modal Test
1	25*L*	0.0073	0.1262
2	25*M*	0.0707	0.2434
3	25*S*	0.2143	0.3753

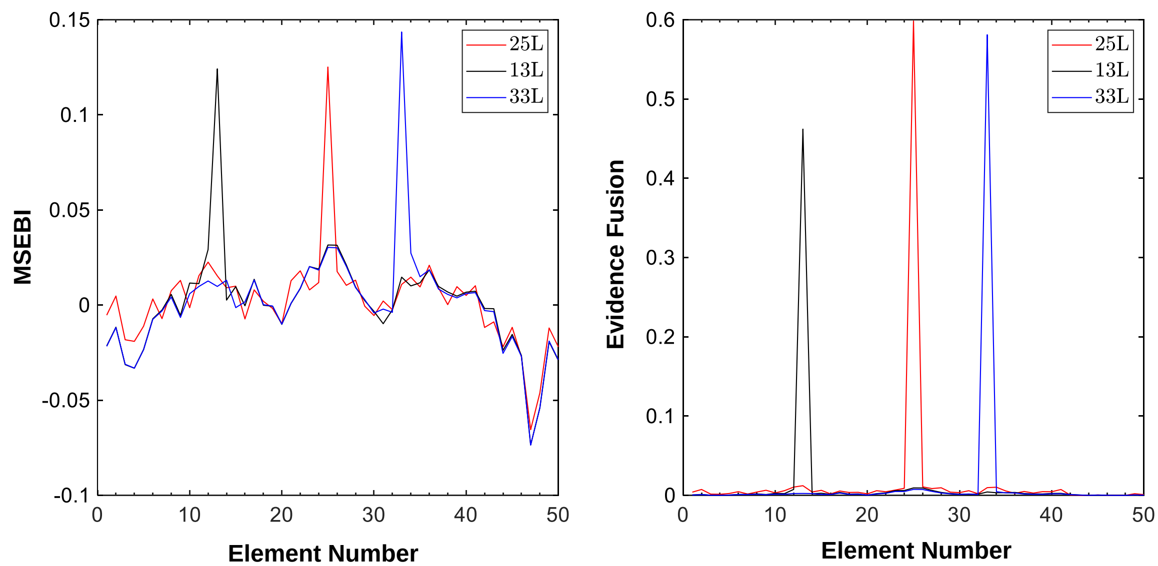

(a) (b)

Fig. 11. The detection results of single damage with the same severity at different locations (a) MSEBI; (b) Evidence fusion FDI

The detection results of modal test coincided with those of the finite element simulation. However, the test data with noise was not as good as the simulation data. Some sharp fluctuations are observed in the MSEBI curves, especially for light damage, which may cause some false peaks. The fusion indicators showed almost the same effectiveness as the results of the finite element simulation.

Based on the results of the finite element modal analysis and modal test, the fusion indicator FDI can accurately detect and locate the damage with different severities, and the MSEBI indicators are sensitive to different damage severities for single damage at the same location. Therefore, the two indicators can be used together in the detection of wooden beams.

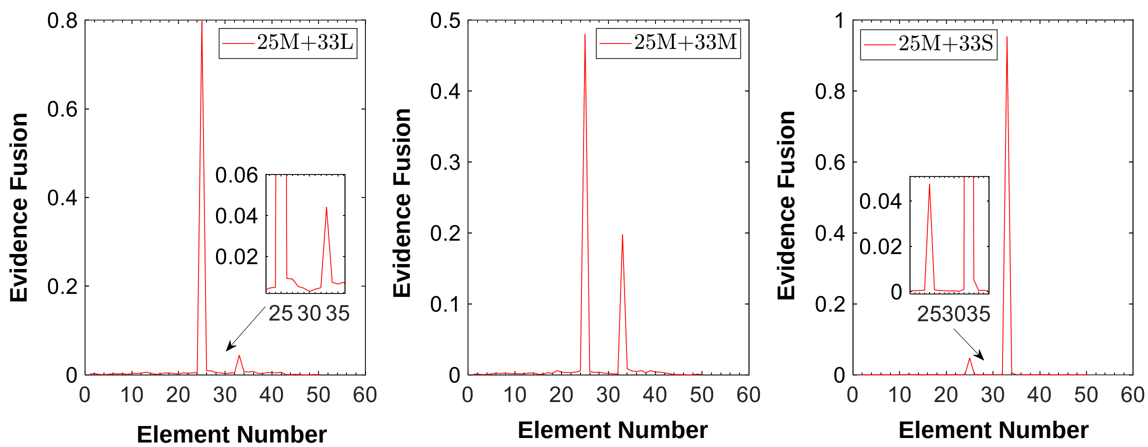

Fig. 12. The detection results of dual damages based on the evidence fusion FDI

CONCLUSIONS

1. The finite element simulation results show that the fused damage indicator proposed in this study based on the modal strain energy change and evidence theory has good anti-noise ability compared with the methods applied in the literature (Hu and Afzal 2006; Hu *et al.* 2011). The procedure can accurately detect and locate the damage with light, medium, or severe severity for single or dual damage detection.
2. The results of the modal test with the same damage cases as the finite element simulation analysis further verify the validity and reliability of the fused damage indicator based on the modal strain energy change and evidence theory for the damage detection of wooden beams.
3. For the single damage at the same location, the MSEBI indicator is more sensitive to damage severity than the FDI indicator. In the actual single damage detection of the same location, the FDI indicator can be used to detect and locate the damage, whereas the MSEBI indicator is then used to analyze the damage severity.
4. The proposed method can also be applied to multiple damage detection, which provides a new practical and effective method for the damage detection of the wooden beams.

ACKNOWLEDGMENTS

This research was financially supported by the Priority Academic Program Development of Jiangsu Higher Education Institutions (PAPD).

REFERENCES CITED

Choi, F. C., Li, J., Samali, B., and Crews, K. (2007). "Application of modal-based damage-detection method to locate and evaluate damage in timber beams," *Journal of Wood Science* 53(5), 394-400. DOI: 10.1007/s10086-006-0881-5

Fei, Q., Li, A., and Han, X. (2009). "Simulation study on damage localization of a beam using evidence theory," *Procedia Engineering* 1(1), 147-150. DOI: 10.1016/j.proeng.2009.06.034

Ghiasi, R., Ghasemi, M. R., and Noori, M. (2018). "Comparative studies of metamodeling and Ai-based techniques in damage detection of structures," *Advances in Engineering Software* 125, 101-112. DOI: 10.1016/j.advengsoft.2018.02.006

Hu, C., and Afzal, M. T. (2006). "A statistical algorithm for comparing mode shapes of vibration testing before and after damage in timbers," *Journal of Wood Science* 52(4), 348-352. DOI: 10.1007/s10086-005-0769-9

Hu, C., Xiao, M., Zhou, H., Wen, W., and Yun, H. (2011). "Damage detection of wood beams using the differences in local modal flexibility," *Journal of Wood Science* 57(6), 479-483. DOI: 10.1007/s10086-011-1200-3

Khosravan, A., Asgarian, B., and Shokrgozar, H. R. (2021). "Improved modal strain energy decomposition method for damage detection of offshore platforms using data of sensors above the water level," *Ocean Engineering* 219, article ID 108337. DOI: 10.1016/j.oceaneng.2020.108337

Kim, J.-T., Ryu, Y.-S., Cho, H.-M., and Stubbs, N. (2003). "Damage identification in beam-type structures: Frequency-based method *vs* mode-shape-based method," *Engineering Structures* 25(1), 57-67. DOI: 10.1016/S0141-0296(02)00118-9

Kouroussis, G., Fekih, L. B., and Descamps, T. (2017). "Assessment of timber element mechanical properties using experimental modal analysis," *Construction and Building Materials* 134, 254-261. DOI: 10.1016/j.conbuildmat.2016.12.081

Liu, G., Zhai, Y., Leng, D., Tian, X., and Mu, W. (2017). "Research on structural damage detection of offshore platforms based on grouping modal strain energy," *Ocean Engineering* 140, 43-49. DOI: 10.1016/j.oceaneng.2017.05.021

Pandey, A., Biswas, M., and Samman, M. (1991). "Damage detection from changes in curvature mode shapes," *Journal of Sound and Vibration* 145(2), 321-332. DOI: 10.1016/0022-460X(91)90595-B

Qin, W., Zhao, J., Shi, M., Yin, G., Lian, X., Wang, L., and Yepes, V. (2020). "Damage localization based on modal strain energy index and evidence theory," *E3S Web of Conferences* 165, article ID 06053. DOI: 10.1051/e3sconf/202016506053

Shi, Z., Law, S., and Zhang, L. (1998). "Structural damage localization from modal strain energy change," *Journal of Sound and Vibration* 218(5), 825-844. DOI: 10.1006/jsvi.1998.1878

Teng, S., Chen, G., Liu, G., Lv, J., and Cui, F. (2019). "Modal strain energy-based structural damage detection using convolutional neural networks," *Applied Sciences* 9(16), article 3376. DOI: 10.3390/app9163376

Wang, S., and Xu, M. (2019). "Modal strain energy-based structural damage identification: A review and comparative study," *Structural Engineering International* 29(2), 234-248. DOI: 10.1080/10168664.2018.1507607

Yang, X., Amano, T., Ishimaru, Y., and Iida, I. (2003). "Application of modal analysis by transfer function to nondestructive testing of wood II: Modulus of elasticity evaluation of sections of differing quality in a wooden beam by the curvature of the flexural vibration wave," *Journal of Wood Science* 49(2), 140-144. DOI: 10.1007/s100860300022

Yang, X., Ishimaru, Y., Iida, I., and Urakami, H. (2002). "Application of modal analysis by transfer function to nondestructive testing of wood I: Determination of localized defects in wood by the shape of the flexural vibration wave," *Journal of Wood Science* 48(4), 283-288. DOI: 10.1007/BF00831348

Zhang, R., Chang, H., Li, Z., Song, X., Yang, J., and Xia, J. (2022). "Corrosion damage identification of towering steel headframe based on parametric modeling and data fusion," *Buildings* 12(8), article 1215. DOI: 10.3390/buildings12081215

Article submitted: October 21, 2022; Peer review completed: May 27, 2023; Revised version received: May 30, 2023; Accepted: May 31, 2023; Published: June 9, 2023.
DOI: 10.15376/biores.18.3.5133-5145